

Democratic parameterization and analysis for 331 model as a subgroup of $SU(6)$

Rena Çiftçi,^a Abbas Kenan Çiftçi,^b and Oleg Popov^{c,d,1}

^a*Department of Physics, Faculty of Science, Ege University, 35040 Bornova, Izmir, Türkiye*

^b*Department of Physics, Faculty of Arts and Sciences, Izmir University of Economics, 35330 Balçova, Izmir, Türkiye*

^c*Department of Biology, Shenzhen MSU-BIT University, 1, International University Park Road, Shenzhen 518172, China*

^d*Department of Physics, Korea Advanced Institute of Science and Technology, 291 Daehak-ro, Yuseong-gu, Daejeon 34141, Republic of Korea*

E-mail: rena.ciftci@ege.edu.tr, kenan.ciftci@ieu.edu.tr, opopo001@ucr.edu

ABSTRACT: A democratic parameterization is introduced for $SU(3)_C \otimes SU(3)_L \otimes U(1)_X$ extension of the Standard Model, which is inspired by $SU(6)$ symmetry. In the novel scenario all Cabibbo-Kobayashi-Maskawa mixing angles and quark masses, nine observable quantities in total, are predicted within 1–3 standard deviations of the experimental values with a minimum number of input parameters. The present work provides the thorough numerical analysis and correlations between input parameters and predicted quantities. $\chi^2 \approx 0.67$ with $\forall \sigma < 0.61$ corresponds to the best global fit benchmark point. Benefits of the new parameterization and future prospects are discussed as well.

KEYWORDS: 331 model, quark mass, CKM, mixing, parameterization

ARXIV EPRINT: [2212.xxxx](https://arxiv.org/abs/2212.00282)

¹Corresponding author.

Contents

1	Introduction	1
2	331 Model	2
2.1	Quark content of Variant-B	3
2.2	Higgs and New Gauge Bosons	3
2.3	Democratic Approach to the Quark Sector of 331 Model	4
3	Parameterization of the Model	6
4	Numerical analysis	7
5	Results	15
6	Discussion	17
7	Conclusion	18

1 Introduction

Although the Standard Model (SM) is effective in accurately describing all fundamental forces excluding the gravity, it suffers from large mass spectra and fermionic hierarchies, small quark mixing angles, and the existence of three fermion generations, violation of CP, etc. A number of extensions to SM have been considered to address some of these issues. The so-called 331 model is one of the simplest extensions that change the electroweak gauge group of SM from $SU(3)_C \otimes SU(2)_L \otimes U(1)_Y$ to $SU(3)_C \otimes SU(3)_L \otimes U(1)_X$. Initially, these models were presented as a natural explanation for the number of fermionic families observed in nature.

Many research have focused on the 331 based model, which was inspired by the need to solve issues in numerous phenomenological applications. For example, papers on 331 model include, but not limited to, applications in neutrino mass generation [1, 2], flavour physics [3–6], and another phenomenological challenges [7–16]. Beyond that, taking into account by now well recognized W boson mass anomaly, reported earlier this year by the Collider Detector at Fermilab (CDF) Collaboration obtained at Tevatron particle accelerator [17], probable interconnection between W mass anomaly and the super-symmetric version of the 331 model has been studied [18]. For more up to date articles on 331 models check [19–22]. From another side, models based on 331 gauge group may be interpreted as a forerunner to grand unification models at high energy scales [23–25]. At last, 3311 model, an extended alternative of the 331 model, has been studied in the context with neutrino mass generation mechanism and dark matter candidates [26–29].

Various variations of the 331 type have been studied in detail so far. This model can be made anomaly free in a variety of ways. Model 331 can be made anomaly free within the family like SM. Alternatively, other variants can use all three families and be anomaly free. The second approach is very attractive because it naturally explains SM's family number of three.

In a recent article submitted by authors of the present paper [30], Democratic Mass Matrix (DMM) approach has been applied to $SU(3)_C \otimes SU(3)_L \otimes U(1)_X$ extension of the SM inspired by E_6 symmetry. The model, named as Variant-A, is anomaly free per generation of quarks and leptons [31]. In the same work, another anomaly free model in quark/lepton generation, named as Variant-B, is given as $SU(3)_C \otimes SU(3)_L \otimes U(1)_X$ extension of the SM and is inspired by both $SU(6)$ [32] and $SU(6) \otimes U(1)_X$ [33] symmetries. While Variant-A has additional (isosinglet) quarks in down sector, Variant-B has additional (isosinglet) quarks in up sector. Details of the latter variant are given in Ref. [34].

Introductory literature on 331 models and DMM approach can be reached in our mentioned paper [30]. Yukawa coupling constants of the weak interaction Lagrangian are assumed by DMM to be about the same. Fermions acquire various masses as a result of the small deviations from the full democratic mass matrices through calculation of mass eigenvalues. The democratic parameterization of Variant-A was very successful to fit into the recent experimental data [35] on quark masses and CKM mixing matrix at the scale of mass of Z boson [30]. In this study, we want to confirm that the same parameterization works for the Variant-B of 331 model as well. Since a summary of motivation and short history of the DMM approach and 331 Model is given in our earlier paper, we will not go over it again.

The structure of the paper is as follows: The quark content and new gauge bosons, neutral and charged currents, DMM parameterization of the variation B of the 331 model are given in Section 2. Section 3 contains details and definition of the new parameterization for the B variant. Numerical analysis and generated correlation graphs are given in section 4. Analysis results, more precisely the input parameters and obtained observable variables for the three most important and relevant benchmark points are presented in section 5. Future prospects and features of the collected results are discussed in Section 6. Conclusion is given in section 7.

2 331 Model

The model with $SU(3)_C \otimes SU(3)_L \otimes U(1)_X$ electroweak gauge group is one of the minimal extensions of SM. It is possible to envisage various sub-models of this model with no exotic electrically charged particles [34]. Triangle anomalies can be eliminated throughout each generation. In fact, one of these models (Variant-A) was taken into consideration by the authors of this work in an earlier paper. Since this study's focus is on the prospect of democratic parameterization of another model (Variant-B) with anomalies canceling in each generation independently, a brief overview of the model's quark sector, charged currents, and neutral currents is provided in this sub-section.

2.1 Quark content of Variant-B

The quark structure for this model [34] is as following:

$$Q_L^\alpha = \begin{pmatrix} u_\alpha \\ d_\alpha \\ U_\alpha \end{pmatrix}_L \quad u_{\alpha L}^c \quad d_{\alpha L}^c \quad U_{\alpha L}^c, \quad (2.1)$$

$$\{3, 3, \frac{1}{3}\} \quad \{3^*, 1, -\frac{2}{3}\} \quad \{3^*, 1, \frac{1}{3}\} \quad \{3^*, 1, -\frac{2}{3}\}$$

where $\alpha = 1, 2, 3$ correspond to the three families. Numbers in parenthesis refer to $(SU(3)_C, SU(3)_L, U(1)_X)$ quantum numbers, where X arising in the electric charge generators of the gauge group is defined as

$$Q = \frac{1}{2}\lambda_{3L} + \frac{1}{2\sqrt{3}}\lambda_{8L} + XI_3, \quad (2.2)$$

where λ_{iL} ($i = 1, \dots, 8$) are Gell-Mann matrices for $SU(3)_L$ and I_3 is 3-dimensional identity matrix.

2.2 Higgs and New Gauge Bosons

Model contains three Higgs fields, which are $(\phi_1^-, \phi_1^0, \phi_1'^0)$, $(\phi_2^-, \phi_2^0, \phi_2'^0)$ and $(\phi_3^0, \phi_3^+, \phi_3'^+)$. Vacuum Expectation Values (VEV) of Higgs fields are the following:

$$\begin{aligned} \langle \phi_1 \rangle &= (0, 0, M)^T, \\ \langle \phi_2 \rangle &= (0, \frac{\eta}{\sqrt{2}}, 0)^T, \\ \langle \phi_3 \rangle &= (\frac{\eta'}{\sqrt{2}}, 0, 0)^T, \end{aligned} \quad (2.3)$$

where $\eta \sim 250$ GeV ($\eta' = \eta$ can be taken for simplicity).

Moreover, there are a total of 17 gauge bosons in this model. One of the gauge fields is the gauge boson associated with $U(1)_X$. Eight of them are associated with $SU(3)_C$. Gauge bosons of W^\pm , K^\pm , K^0 and \bar{K}^0 are responsible from the charged current in the electroweak sector. Z and Z' bosons are given for neutral current, which are also massive and uncharged. The masses of the new bosons are proportional to the symmetry breaking scale of the model (order of a few TeV). The masses of the gauge bosons of the electroweak sector can be obtained with the help of expressions below:

$$m_{W^\pm}^2 = \frac{g^2}{4}(\eta^2 + \eta'^2), \quad (2.4a)$$

$$m_Z^2 = \frac{m_{W^\pm}^2}{C_W^2}, \quad (2.4b)$$

$$m_{K^\pm}^2 = \frac{g^2}{4}(2M^2 + \eta'^2), \quad (2.4c)$$

$$m_{K^0(\bar{K}^0)}^2 = \frac{g^2}{4}(2M^2 + \eta^2), \quad (2.4d)$$

$$m_{Z'}^2 = \frac{g^2}{4(3 - 4S_W^2)} \left[8C_W^2 M^2 + \frac{\eta^2}{C_W^2} + \frac{\eta^2(1 - 2S_W^2)^2}{C_W^2} \right], \quad (2.4e)$$

where cosine and sine of the Weinberg angle are abbreviated by C_W and S_W , respectively, and $S_W^2 = 0.23122$ as an experimental value. An important note is that there are five new gauge bosons beyond those of the SM. The masses of these BSM bosons can be tested in the bounds of the Large Hadron Collider (LHC) detectors. This is possible because TeV order mass values for these BSM bosons are still with an allowed parameter window. These gauge bosons' mass value constraints have been set by the non-observation of the specific kinds of the LHC events [36], that were expected to be detected. A more up-to-date and more strict limit of the Z' boson's mass is fixed at $M_{Z'} > 5.1$ TeV and $M_{Z'} > 4.6$ TeV at 95% CL. This was determined by using the most recent ATLAS [37] and CMS data [38], respectively.

In reality, the involvement of additional heavy gauge bosons [36], the charged ones often represented by W' , is the characteristic shared by many models produced by expanding the SM. By resonantly producing fermion or electroweak boson pairs, W' bosons would be seen in the LHC. A large amount of lost transverse energy and a high-energy electron or muon make up the most widely considered signature. At the moment, the stringent limits on the W' 's mass are set at $M_{W'} > 6$ TeV with 95% CL [39], under an assumption of the coupling between SM fermions and model's BSM gauge bosons. Despite the fact that this restriction have no direct effect on the model under consideration, nonetheless, it acts as a guide for the K^\pm and K^0 bosons' mass values.

The model's Charged Currents (CC) are expressed as follows

$$\begin{aligned} \mathcal{L}_{CC} = & -\frac{g}{\sqrt{2}} [\bar{\nu}_L^\alpha \gamma^\mu e_L^\alpha W_\mu^+ + \bar{N}_L^\alpha \gamma^\mu e_L^\alpha K_\mu^+ + \bar{\nu}_L^\alpha \gamma^\mu N_L^\alpha K_\mu^0 + \bar{u}_{\alpha L} \gamma^\mu d_{\alpha L} W_\mu^+ \\ & + \bar{U}_{\alpha L} \gamma^\mu d_{\alpha L} K_\mu^+ - \bar{U}_{\alpha L} \gamma^\mu u_{\alpha L} K_\mu^0 + \text{h.c.}] , \end{aligned} \quad (2.5)$$

and neutral currents (NC) are given by

$$\mathcal{L}^{NC} = -\frac{g}{2C_W} \sum_f [\bar{f} \gamma^\mu (g'_V + g'_A \gamma^5) f Z'_\mu] , \quad (2.6)$$

where f stands for SM quarks and leptons; g , g'_V , and g'_A are the SM and BSM gauge coupling constants of $SU(3)_L$ symmetry's gauge bosons after its Spontaneous Symmetry Breaking (SSB).

From the above expression, we can see that K^\pm BSM gauge bosons mediate transitions between SM down type quarks and BSM isosinglet U type quarks, where as the interactions between SM up type quarks and BSM isosinglet U type quarks are mediated by K^0 and \bar{K}^0 BSM gauge bosons.

2.3 Democratic Approach to the Quark Sector of 331 Model

The Democratic Mass Matrix (DMM) technique was created by H. Harari and H. Fritzsch [40–44] to solve the issues of mass hierarchy and mixings, however it was unable to correctly predict the mass of the top quark. A number of publications were published that addressed this issue by using DMM to four families of SM [45, 46]. ATLAS and CMS data [47, 48] later ruled out the SM type fourth family fermions. As a result, if the DMM technique is right, it will invariably be applied to an extension of the SM. DMM presumes that

the Yukawa coupling constants in the weak interaction Lagrangian are nearly the same. Fermions acquire distinct masses when the mass eigenstates are activated [49–51].

When discussing democracy of 331 model, two different basis are defined: $SU(3)_L \otimes U(1)_X$ symmetry basis, labeled with superscript “(0)” as in $f^{(0)}$ and the mass basis labeled without superscript as in f , where f stands for any fermion particle. Applying the DMM technique to the Variant-B, before breaking the electroweak spontaneous symmetry (EWSS), quarks are organized as follows:

$$\begin{pmatrix} u^{(0)} \\ d^{(0)} \\ U^{(0)} \end{pmatrix}_L, \quad u_L^{c(0)}, d_L^{c(0)}, U_L^{c(0)}, \quad (2.7a)$$

$$\begin{pmatrix} c^{(0)} \\ s^{(0)} \\ C^{(0)} \end{pmatrix}_L, \quad c_L^{c(0)}, s_L^{c(0)}, C_L^{c(0)}, \quad (2.7b)$$

$$\begin{pmatrix} t^{(0)} \\ b^{(0)} \\ T^{(0)} \end{pmatrix}_L, \quad t_L^{c(0)}, b_L^{c(0)}, T_L^{c(0)}. \quad (2.7c)$$

All bases are equivalent in the case of one-family. The Lagrangian with the quark Yukawa terms for a one-family situation can be expressed as follows:

$$\mathcal{L}_y^Q = Q_L^T C (a_d \phi_2 d_L^c + a_u \phi_3 u_L^c + a_U \phi_1 U_L^c + a_{uU} \phi_3 U_L^c + a_{Uu} \phi_1 u_L^c) + h.c., \quad (2.8)$$

where a_d , a_u , a_U , a_{uU} and a_{Uu} are Yukawa couplings in the $SU(3)_L \otimes U(1)_X$ basis and C is the charge conjugate operator.

In this case, we obtain a mass term for the down-quark sector:

$$m_d^0 = a_d \frac{\eta^d}{\sqrt{2}} \quad (\eta^d = \eta^u = \eta \text{ is taken for simplicity}), \quad (2.9)$$

and a mass term for the up-quark sector is given as:

$$m_{uU}^0 = \begin{pmatrix} a_u \eta^u / \sqrt{2} & \varepsilon a_u \eta^u / \sqrt{2} \\ \varepsilon a_U \eta^U / \sqrt{2} & a_U \eta^U / \sqrt{2} \end{pmatrix}, \quad (2.10)$$

where ε is chosen very close to one, and εa_u corresponds to the a_{uU} and εa_U corresponds to the a_{Uu} .

To get mass eigenvalues, we need to diagonalize the mass matrix above. This is done in Ref. [52] to show that this technique gives the correct t and b quark masses in the case of one-family.

Now, we are able to write three-family quark Yukawa Lagrangian in the $SU(3)_L \otimes U(1)_X$ basis:

$$\begin{aligned}
\mathcal{L}_y^Q = & \sum_{i=1}^3 Q_L^{iT} C(a_d \phi_2 d_L^c + a_u \phi_3 u_L^c + a_U \phi_1 U_L^c + \varepsilon a_u \phi_3 U_L^c + \varepsilon a_U \phi_1 u_L^c) \\
& + \sum_{i=1}^3 Q_L^{iT} C(a_s \phi_2 s_L^c + a_c \phi_3 c_L^c + a_C \phi_1 C_L^c + \varepsilon a_c \phi_3 C_L^c + \varepsilon a_C \phi_1 c_L^c) \\
& + \sum_{i=1}^3 Q_L^{iT} C(a_b \phi_2 b_L^c + a_t \phi_3 t_L^c + a_T \phi_1 T_L^c + \varepsilon a_t \phi_3 T_L^c + \varepsilon a_T \phi_1 t_L^c) + \text{h.c.}
\end{aligned} \tag{2.11}$$

3 Parameterization of the Model

Every quark mass matrix has a little variation, symbolized by parameters labeled as β and γ , which breaks the democratic pattern. The shape of the deviation for down, up, and heavy up BSM quarks comprises identical structure. Nevertheless, separate parameter sets are used to parameterize variances. The following are the quark mass matrices of down, up, and heavy up BSM isosinglet sectors

$$\mathcal{M}_u^0 = \frac{a^u \eta^u}{\sqrt{2}} \begin{pmatrix} 1 + \gamma_u & 1 & 1 - \frac{9}{2} \gamma_u + \beta_u \\ 1 & 1 - 2\gamma_u & 1 + 3\gamma_u + \beta_u \\ 1 - \frac{9}{2} \gamma_u + \beta_u & 1 + 3\gamma_u + \beta_u & 1 + 4\beta_u \end{pmatrix}, \tag{3.1a}$$

$$\mathcal{M}_d^0 = \frac{a^d \eta^d}{\sqrt{2}} \begin{pmatrix} 1 + \gamma_d & 1 & 1 - \frac{9}{2} \gamma_d + \beta_d \\ 1 & 1 - 2\gamma_d & 1 + 3\gamma_d + \beta_d \\ 1 - \frac{9}{2} \gamma_d + \beta_d & 1 + 3\gamma_d + \beta_d & 1 + 4\beta_d \end{pmatrix}, \tag{3.1b}$$

$$\mathcal{M}_U^0 = \frac{a^U \eta^U}{\sqrt{2}} \begin{pmatrix} 1 + \gamma_U & 1 & 1 - \frac{9}{2} \gamma_U + \beta_U \\ 1 & 1 - 2\gamma_U & 1 + 3\gamma_U + \beta_U \\ 1 - \frac{9}{2} \gamma_U + \beta_U & 1 + 3\gamma_U + \beta_U & 1 + 4\beta_U \end{pmatrix}. \tag{3.1c}$$

In addition, quarks of the up sector and BSM isosinglet up quarks mix with each other, and the mixing is parameterized by ε parameter according to Eq. (2.11):

$$\mathcal{M}_{uU}^0 = \begin{pmatrix} \mathcal{M}_u^0 & \varepsilon_u \mathcal{M}_u^0 \\ \varepsilon_u \mathcal{M}_u^0 & \mathcal{M}_U^0 \end{pmatrix}. \tag{3.2}$$

\mathcal{M}_{uU}^0 on the $SU(3)_L \otimes U(1)_X$ basis, 6×6 mass matrix diagonalization, generates masses of up SM and Beyond Standard Model (BSM) isosinglet quarks on the mass basis. This mass matrix can be diagonalized with the help of a 6×6 unitary matrix U_{uU} . While down sector quark masses are obtained by diagonalizing \mathcal{M}_d^0 mass matrix with a 3×3 unitary matrix U_d . In a similar manner, 3×3 mixing matrices, U_u and U_U , for up type SM and heavy BSM quarks, respectively, are defined as unitary matrices that diagonalize u and U blocks of the \mathcal{M}_{uU}^0 given in Eq. (3.2). For simplicity, CP violating phases are considered to be zero from now on. As a result, diagonalizing matrices are real orthogonal matrices.

The mixing matrices V_{CKM}^W , V^{K^\pm} and V^{K^0} correspond to W boson of SM, whereas K^\pm and K^0 are heavy BSM gauge bosons, respectively. These mixing matrices are defined through a combinations of 3×3 diagonalizing matrices U_u , U_d , and U_U , mentioned above, and are given by

$$V_{CKM}^W = U_u U_d^T = \begin{pmatrix} V_{ud} & V_{us} & V_{ub} \\ V_{cd} & V_{cs} & V_{cb} \\ V_{td} & V_{ts} & V_{tb} \end{pmatrix}, \quad (3.3a)$$

$$V^{K^\pm} = U_U U_d^T = \begin{pmatrix} V_{Ud} & V_{Us} & V_{Ub} \\ V_{Cd} & V_{Cs} & V_{Cb} \\ V_{Td} & V_{Ts} & V_{Tb} \end{pmatrix}, \quad (3.3b)$$

$$V^{K^0} = U_U U_u^T = \begin{pmatrix} V_{Uu} & V_{Uc} & V_{Ut} \\ V_{Cu} & V_{Cc} & V_{Ct} \\ V_{Tu} & V_{Tc} & V_{Tt} \end{pmatrix}. \quad (3.3c)$$

These matrices can be parameterized with three mixing angles and one phase angle:

$$V = \begin{pmatrix} c_{12}c_{13} & s_{12}c_{13} & s_{13}e^{-i\delta} \\ -s_{12}c_{23} - c_{12}s_{23}s_{13}e^{i\delta} & c_{12}c_{23} - s_{12}s_{23}s_{13}e^{i\delta} & s_{23}c_{13} \\ s_{12}s_{23} - c_{12}c_{23}s_{13}e^{i\delta} & -c_{12}s_{23} - s_{12}c_{23}s_{13}e^{i\delta} & c_{23}c_{13} \end{pmatrix}, \quad (3.4)$$

here $s_{ij} \equiv \sin(\theta_{ij})$, $c_{ij} \equiv \cos(\theta_{ij})$, θ_{ij} are the mixing angles, and δ is CP violating phase(not taken into account in the present work).

4 Numerical analysis

The analysis performed over the model parameterization can be divided into three stages: a systematic scan over all, seven in total (for details see Tab. 1), input parameters of the model, next a more fine grained scan near the points with minimal deviation from the experimental data is performed, then the obtained results were used as a input data for the neural network (NN) training, and further, for obtaining a complete scan over input parameter range. Following the numerical scans, the correlation analyses between different input parameters, distinctive input parameters and predicted observable variables, as well as between various output observable variables was performed. The purpose of studying these correlations is to increase the predictive power of the model and assist in probing the model in the current and future phenomenological experiments. Included below are some of the most important and relevant correlations between input parameters and/or observable variables. The task of the present section is to study the origin behind these correlations.

Results shown below were obtained with the following values for a and η (defined in

Sec. 2.3) parameters

$$\frac{a^u \eta^u}{\sqrt{2}} = 2400 \text{ GeV}, \quad (4.1a)$$

$$\frac{a^d \eta^d}{\sqrt{2}} = 0.91 \text{ GeV}, \quad (4.1b)$$

$$\frac{a^U \eta^U}{\sqrt{2}} = 2.4 \times 10^4 \text{ GeV}. \quad (4.1c)$$

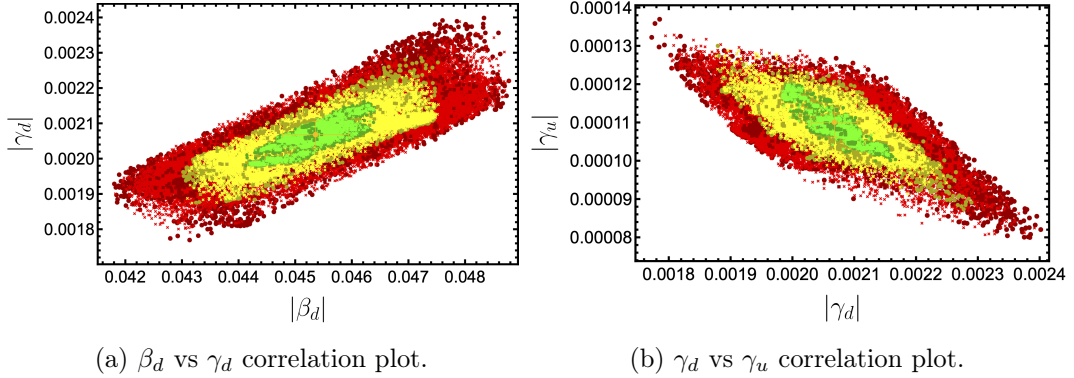


Figure 1: Selected input correlation plots. Maximum standard deviation from experimental values is represented by colors. Red, yellow, and green colors are used for the values $\sigma_{\max} < 3, 2$, and 1 , respectively. Whereas, discs, crosses, and squares correspond to $\langle \sigma \rangle / \sigma_{\max}$: $0.5 - 1.0$, $0.33 - 0.5$, $0 - 0.33$, respectively.

The strongest correlation patterns between distinct input parameters are shown in Fig. 1. As can be seen from Fig. 1a, there is direct correlation between β_d and γ_d input parameters. Fig. 1b demonstrates the correlation between γ_u and γ_d , which exhibits an inverse correlation contrary to the β_d vs γ_d case. Both of these behaviours are drastically different from analogous correlation for the Variant A of the 331 model [30]. Other combinations of input parameters exhibit no apparent correlation.

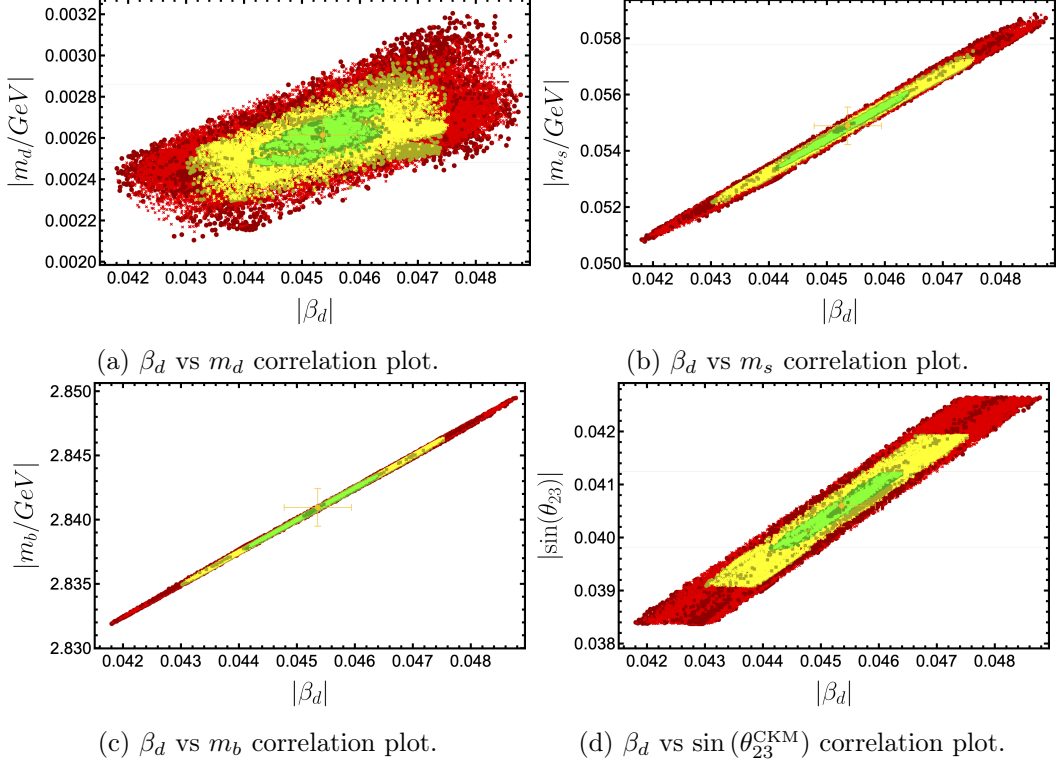
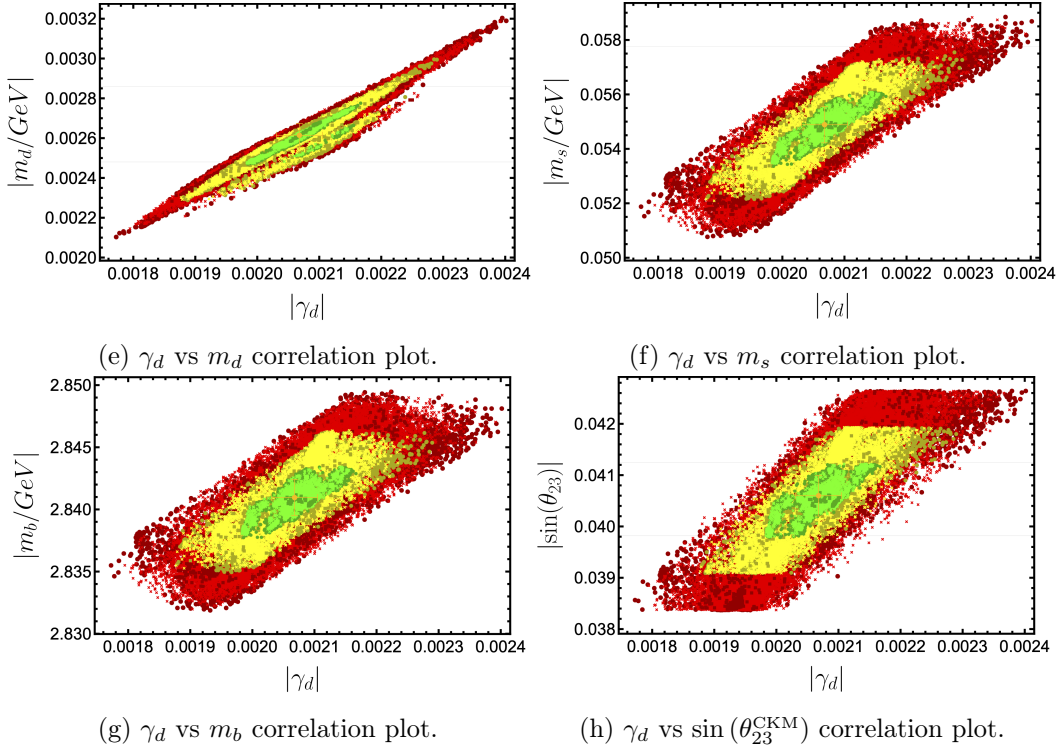


Figure 2: continued.



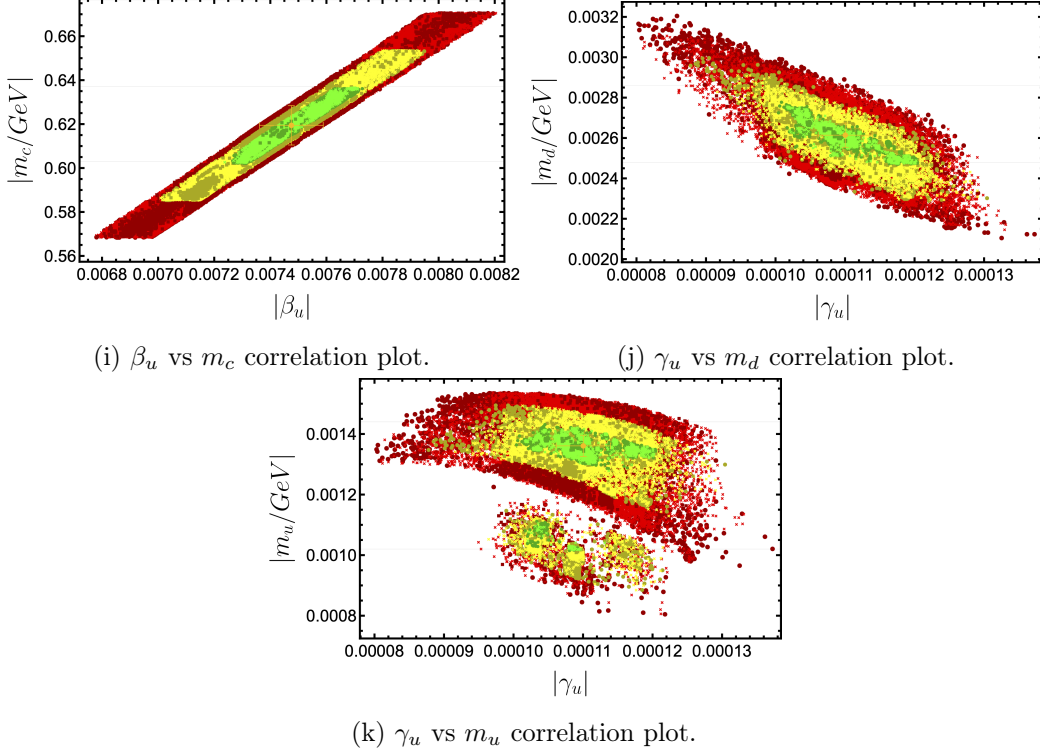


Figure 2: Selected correlation plots between input parameters and observable variables. Grid lines represent areas of the experimental data with one standard deviation. Red, yellow, and green colors are used for the values $\sigma_{\max} < 3$, 2, and 1, respectively. Whereas, discs, crosses, and squares correspond to $\langle \sigma \rangle / \sigma_{\max}$: 0.5–1.0, 0.33–0.5, 0–0.33, respectively.

The plots in the Fig. 2 demonstrate important dependence of some observable variables on model input parameters. For instance, plot in Fig. 2a shows the direct but weak dependence of m_d , lightest eigenvalue of the down quark sector, on the input parameter β_d , compared to the cases with its heavier counterparts of the sector. Strong direct correlations are observed between m_s and β_d , as well as between m_b and β_d (Fig. 2b, 2c). Furthermore, from Fig. 2d one can see that there is a similar linear dependence of $\sin(\theta_{23}^{\text{CKM}})$ on β_d . An analogous correlation can be seen between $\gamma_d - m_d$, $\gamma_d - m_s$, $\gamma_d - m_b$ and $\gamma_d - \sin(\theta_{23}^{\text{CKM}})$ (Fig. 2e, 2f, 2g and Fig. 2h), which exhibit proportional direct-linear behaviour. The direct proportionality between m_d and γ_d can be seen from Eq. (3.1b), for which the lightest eigenvalue (m_d) approaches to zero as γ_d goes to zero. Since m_s and m_b are most sensitive to the β_d their β_d plots are much thinner compared to their plots vs γ_d . Situation with m_d is reversed because γ_d has a leading effect on it. Similar to the situation in the down sector Fig. 2b, β_u has a strongest influence on the m_c , Fig. 2i, with a direct-linear behaviour. Furthermore, an inverse proportionality between m_d and γ_u , which is depicted in Fig. 2j, is originated from indirect relation between up and down sectors through the CKM mixing angles.

From the above analysis it can be concluded that β_d and γ_d have noticeable influence on all the down sector mass eigenvalues and $\sin(\theta_{23}^{\text{CKM}})$, whereas β_u affects up sector quark

masses. The correlation between m_t and β_u is absent due to the mixing of SM up quark sector with BSM heavy quarks. γ_u has the strongest effect on m_u . Fig. 2k demonstrates two minima of m_u with respect to γ_u . Similarly, two minima are observed in other input parameters vs m_u plots. m_u dependence on γ_u is not direct nor linear, unlike the situation with γ_d and m_d (Fig. 2e), this is caused by the affect of ε and mixing of m_u with heavy m_U state. Figs. 2e and 2k contain similar patterns in a sense that patterns consist of two disconnected minimal regions.

Among remarkable correlation patterns of the mixing angles of the CKM matrix are expressed in the $\sin(\theta_{23}^{\text{CKM}})$ mixing angle, proportional linearly and totally constrained by input parameters γ_d and β_d (Fig. 2h and Fig. 2d). Input variables demonstrate more complicated effect on the other CKM mixing angles and therefore will be skipped in the further discussion.

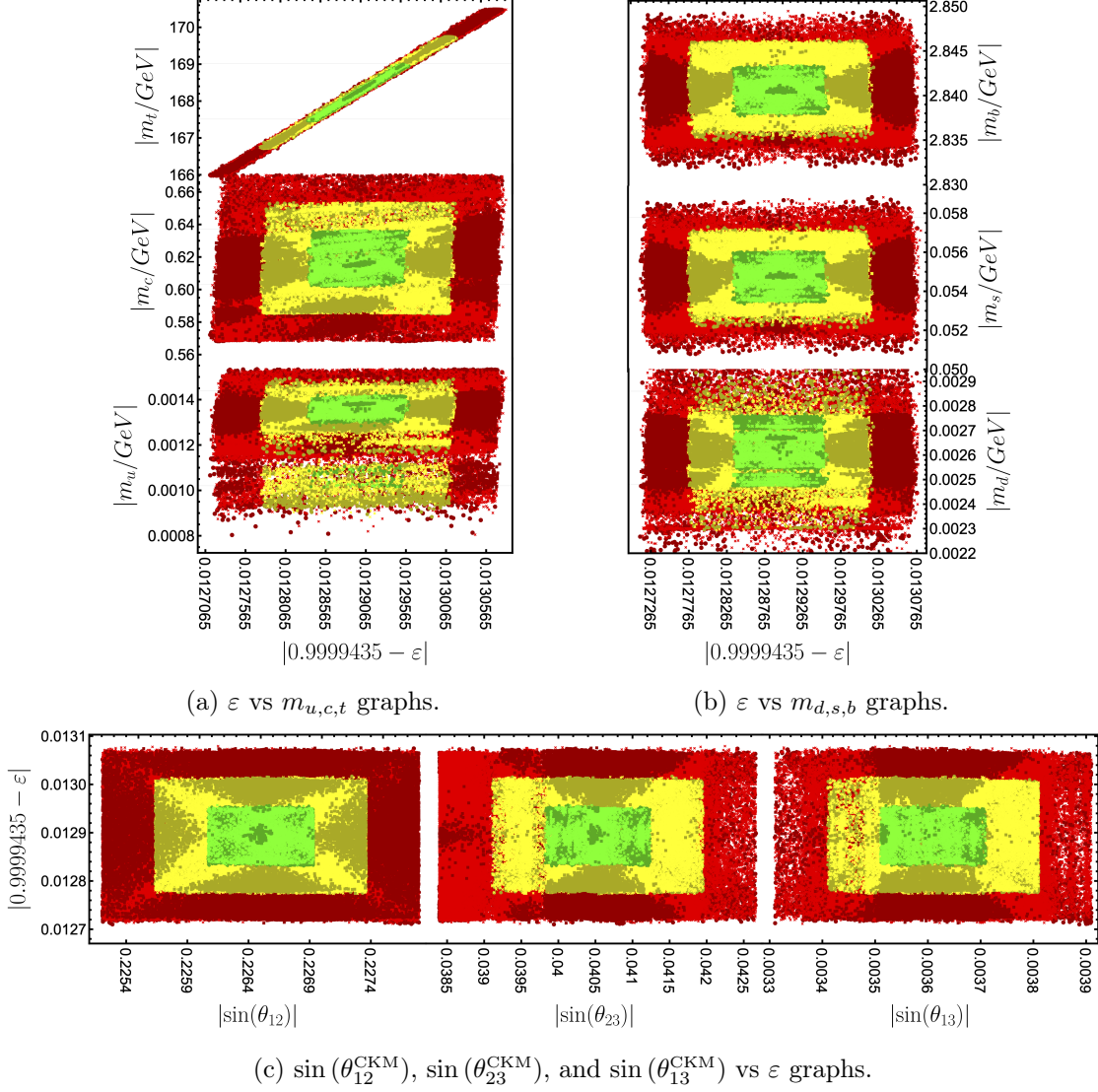


Figure 3: Correlation plots for ε input parameter vs SM mass eigenvalues. Grid lines represent areas of the experimental data with one standard deviation. Red, yellow, and green colors are used for the values $\sigma_{\max} < 3, 2$, and 1 , respectively. Whereas, discs, crosses, and squares correspond to $\langle \sigma \rangle / \sigma_{\max}$: $0.5 - 1.0$, $0.33 - 0.5$, $0 - 0.33$, respectively.

SM fermion masses and CKM mixing angles dependence on the mixing parameter(ε) between SM up quarks and heavy BSM counterparts is depicted in Fig. 3. ε has a unique effect on the mass eigenvalues. For the up sector, the lightest mass eigenvalue, m_u , dominantly depends on the γ_u , whereas dependence of m_c is lead by β_u , and top quark mass, m_t , is linearly dependent on ε , Figs. 3a, in the neighborhood of $\varepsilon \rightarrow 1$ and approaches zero in its limit. This can be easily seen when $\beta_u, \gamma_u \rightarrow 0$ and taking limit $\varepsilon \rightarrow 1$

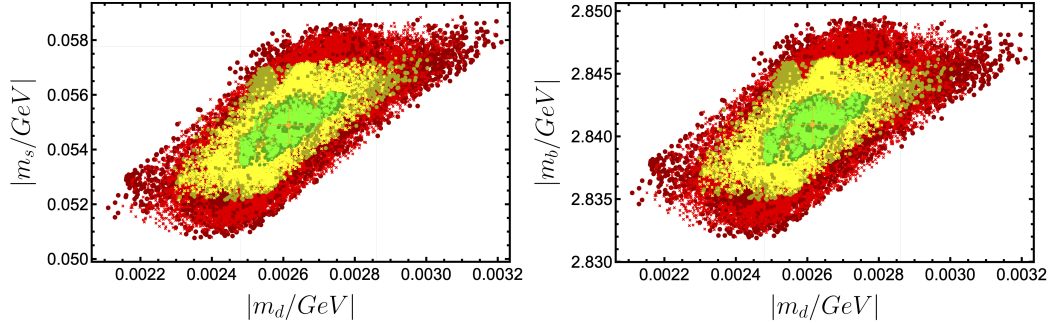
$$m_t = \left(3.96 - \sqrt{10.5 + 5.2\varepsilon^2}\right) \times 10^4 \text{GeV}, \quad (4.2a)$$

$$m_T = \left(3.96 + \sqrt{10.5 + 5.2\varepsilon^2}\right) \times 10^4 \text{GeV}, \quad (4.2b)$$

$$m_t = -1.31 \times 10^4(\varepsilon - 1) \text{GeV}, \quad (4.2c)$$

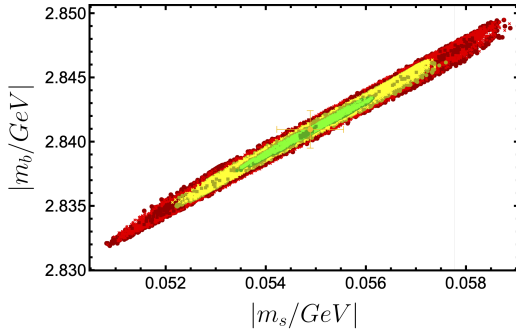
$$m_T = 7.92 \times 10^4 + 1.31 \times 10^4(\varepsilon - 1) \text{GeV}. \quad (4.2d)$$

Since the ε parameter only controls the mixing in the up sector, the down sector practically is independent of it, Figs. 3b. The only indirect effect can be observed via the CKM mixing. Finally, for the CKM mixing angle dependence on ε one can observe indirect relation via the mixing matrix in the up sector. This can be explained in the following way, since top quark mass, m_t , strongly depends on ε , changing which will alter the top quark mass, it will then also shift the values of mixing angles between first two and third family in the up sector, which in return will reveal itself in the CKM mixing matrix, Fig. 3c.

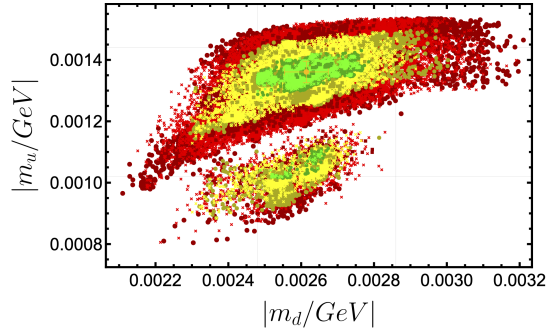


(a) m_d vs m_s global fit distribution graph.

(b) m_d vs m_b global fit distribution graph.



(c) m_s vs m_b global fit distribution graph.



(d) m_d vs m_u global fit distribution graph.

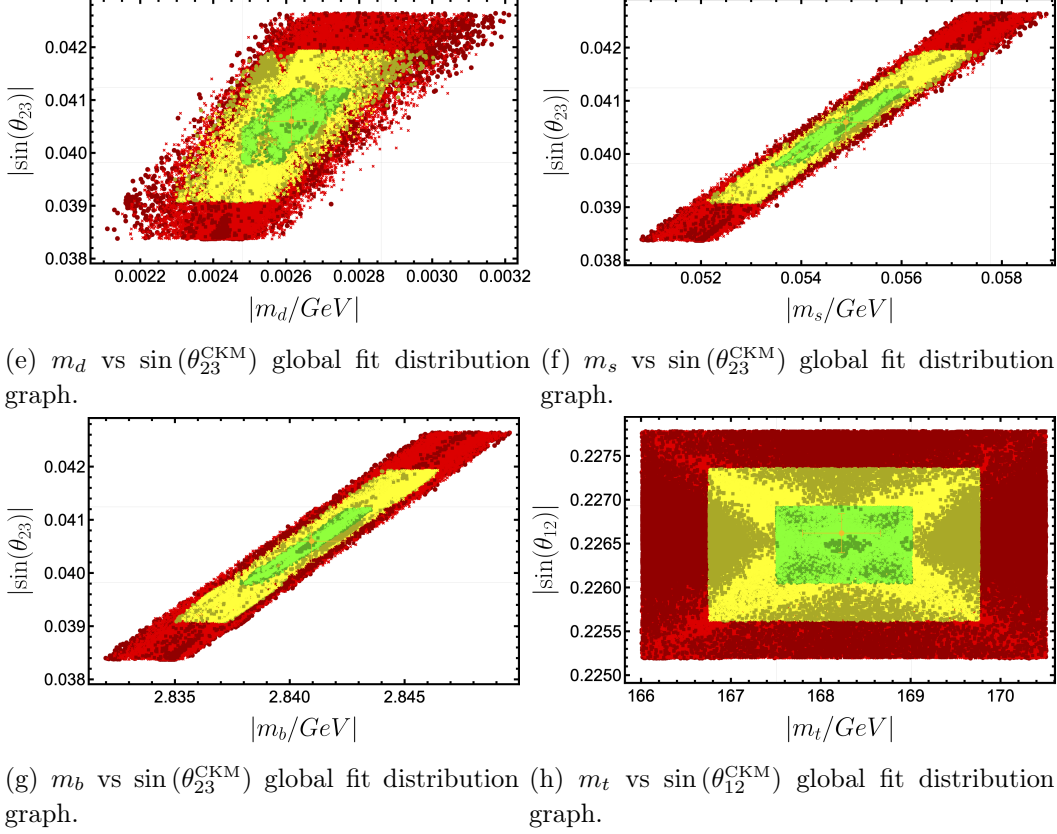


Figure 4: Selected observable correlation plots. Grid lines represent areas of the experimental data with one standard deviation. Red, yellow, and green colors are used for the values $\sigma_{\max} < 3, 2$, and 1 , respectively. Whereas, discs, crosses, and squares correspond to $\langle \sigma \rangle / \sigma_{\max}$: $0.5 - 1.0$, $0.33 - 0.5$, $0 - 0.33$, respectively.

Plots in the Figs. 4a, 4b and 4c demonstrate a direct-linear correlation between all three down sector quark masses. This is an immediate consequence of the fact that all three strongly depend on the β_d input parameter, Figs. 2a, 2b, and 2c. A second local minimum of the best fit of the model in Fig. 4d is the same minimum that appeared in Figs. 2e and 2k.

Figs. 4e, 4f and 4g show the correlations between down quark sector masses and CKM mixing angle, $\sin(\theta_{23}^{\text{CKM}})$. This can be seen immediately from the direct linear dependence of $\sin(\theta_{23}^{\text{CKM}})$ on β_d and γ_d , Fig. 2d and Fig. 2h, respectively. Furthermore, m_d , m_s , and m_b all depend linearly on β_d with various level of strength, Figs. 2a, 2b, and 2c. Finally, in Fig. 4h one can observe a "star"like pattern similar to the one given in the ε vs $\sin(\theta_{12}^{\text{CKM}})$ plot of Fig. 3c. This similarity arises from the linear behaviour of m_t on ε in the limit $\varepsilon \rightarrow 1$, eq.(4.2).

Following the phases assessment in the text succeeding the Eq. (3.2), in the situations when output observable variables were generated with a negative sign, the later was omitted.

5 Results

The results of the model predictions are given and elaborated on in the present section. This interpretation of 331 model, inspired by $SU(6) \otimes U(1)$, anticipates SM up and down quark masses, along with, CKM mixing angles for total of seven input parameters. Down, up and up type BSM isosinglet quark sectors are regulated by two parameters each. In addition, light and massive BSM up quarks are mixed with an additional parameter denoted as ε . The Tab. 1 provides collective list of the input parameters for the three most appropriate and significant benchmark points. The first benchmark point (BP1) is described as a point with the smallest χ^2 of roughly 0.668, which has maximum deviation from experimental results of 0.611σ Eq. (5.1). The second benchmark point (BP2), contrasted with the first, is defined as the position in a parameter space scan with the lowest overall collection of deviations for all nine observable variables at present with a maximum deviation of $\sim 0.487\sigma$. Finally, we give the average of all data points obtained by $\forall \sigma_{\max} \leq 1$ as the third benchmark point (BP3), designated as BP3 _{\langle} in Tab. 1, while the spread (error) of all points contributing to $\forall \sigma_{\max} \leq 1$ is expressed as *Spread*. The deviation σ is described as follows

$$\sigma = \left| \frac{x_{\text{exp}} - x_{\text{th}}}{x_{\text{err}}} \right|, \quad (5.1)$$

here x indicates any of the observable variables from Tab. 2, *exp.* stands for the experimentally obtained value, *th* corresponds to the simulated observable value from the run of the parameter space scan, and lastly, *err.* means the error for the experimentally obtained value.

par.	BP1	BP2	BP3 _{\langle}	BP3 _{spread}
β_d	0.0453747	0.04551359398035038	0.0455525	0.000216767
γ_d	0.00206769	0.0020552844447113165	0.00206312	0.0000139374
β_u	-0.00741599	-0.007358120617229136	-0.00737406	0.0000430917
γ_u	0.000109067	0.00011100359211096111	0.00011017	0.00000139
β_U	0.0491484	0.04924143245126722	0.0492127	0.000405244
γ_U	-0.0300187	-0.030030668585101235	-0.0300332	0.000259112
ε	1.01284	1.012851024748183	1.01268	0.00204506

Table 1: Model input parameters for the several benchmark points given in Tab. 2

Parameter scanning is very sensitive to the precision of input parameter values, so their values are given in Tab. 1 with up to twenty decimal places. The best result for χ^2 for the sum of seven input parameters is given in columns 4 and 5 of the table. 2 with a $\chi^2 \approx 0.668$. As is observed, m_u contributes the most to the χ^2 , but the third generation quark masses of up and down sectors generate a significantly lower imprecision to the χ^2 . Then, as a result of finding the smallest combination of the deviations from the experimental values (2nd and 3rd columns of Tab. 2), the best obtained point is given in the 6th and 7th columns from Tab. 2 with $\chi^2 \approx 1.257$ and $\sigma_{\max} \approx 0.487$. Finally, we collect all points with maximum deviations ($\sigma_{\max} \leq 1$) to generate mean and spread values for the set of the observable variables, given in the 8'th and 9'th column of Tab. 2 with $\chi^2 \approx 1.819$. These numbers

represent the location and size of the region, with deviations from the experimental values smaller than one (green area in Fig. 5).

Observable	Experimental [35]		BP1		BP2		BP3	
	Value	Err.	Value	σ	Value	σ	$\langle \rangle$	Spread
m_d (MeV)	2.67	0.19	2.61	0.30	2.58	0.45	2.60	0.03
m_s (MeV)	53.16	4.61	54.90	0.38	55.02	0.403	55.08	0.24
m_b (GeV)	2.839	0.026	2.841	0.077	2.841	0.091	2.841	0.001
m_u (MeV)	1.23	0.21	1.36	0.61	1.33	0.48	1.34	0.02
m_c (MeV)	620	17	616	0.23	612	0.48	613	3.9
m_t (GeV)	168.26	0.75	168.26	0.0017	168.42	0.21	168.27	0.44
M_U (GeV)	—	—	3109	-	3109	-	3110	33
M_C (GeV)	—	—	4296	-	4298	-	4298	31
M_T (GeV)	—	—	83548	-	83555	-	83551	37
$\sin(\theta_{12})$	0.22650	0.000431	0.22651	0.020802	0.22666	0.36099	0.22654	0.000233
$\sin(\theta_{23})$	0.04053	$^{+0.000821}_{-0.000601}$	0.04056	0.047517	0.04062	0.12329	0.04066	0.000156
$\sin(\theta_{13})$	0.00361	$^{+0.000110}_{-0.000090}$	0.00360	0.063327	0.00366	0.48656	0.00364	0.000035
$\sin(\theta_{12}^{K^\pm})$	—	—	0.79602	-	0.79513	-	0.79544	-
$\sin(\theta_{23}^{K^\pm})$	—	—	0.01713	-	0.01710	-	0.01707	-
$\sin(\theta_{13}^{K^\pm})$	—	—	0.01232	-	0.01235	-	0.01238	-
$\sin(\theta_{12}^{K^0})$	—	—	0.63813	-	0.63688	-	0.63737	-
$\sin(\theta_{23}^{K^0})$	—	—	0.04605	-	0.04607	-	0.04607	-
$\sin(\theta_{13}^{K^0})$	—	—	0.01635	-	0.01635	-	0.01635	-
χ^2	—	—	0.668	—	1.257	—	1.819	—

Table 2: Various benchmark points of the model with the smallest χ^2 , the smallest σ_{\max} , and mean value for $\forall \sigma_{\max} \leq 1$; where σ is the standard deviation and has no units, Eq. (5.1). The obtained values shown above have been rounded to have the same significant numbers as the experimental results.

The masses and mixing angles in Tab. 2 were defined as eigenvalues of mass matrices in Eqs. (3.1b), (3.2), and as in Eq. (3.4) for V_{CKM}^W (Eq. (3.3a)), V^{K^\pm} (Eq. (3.3b)), V^{K^0} (Eq. (3.3c)), respectively.

Figure 5 summarizes all the data points collected during input parameter space scan according to two criteria: horizontal axis corresponds to σ_{\max} which represents the maximum deviation of each data point with respect to the experimental value obtained up to date, whereas the vertical axis shows the corresponding χ^2 values for each data point obtained. The plot in Fig. 5 is divided vertically into three horizontal regions according to the value of σ_{\max} : $0 - 1$, $1 - 2$, $2 - 3$; vertical region is separated into three categories as well, according to the values of $\langle \sigma \rangle / \sigma_{\max}$: $0 - 0.33$, $0.33 - 0.5$, $0.5 - 1.0$. The subdivision according to the last category represents the spread of all errors that contribute the total χ^2 . The solid curves on the plot stand for upper and lower theoretical limits for this plot given by $\chi^2 = 9\sigma_{\max}^2$ and $\chi^2 = \sigma_{\max}^2$, respectively.

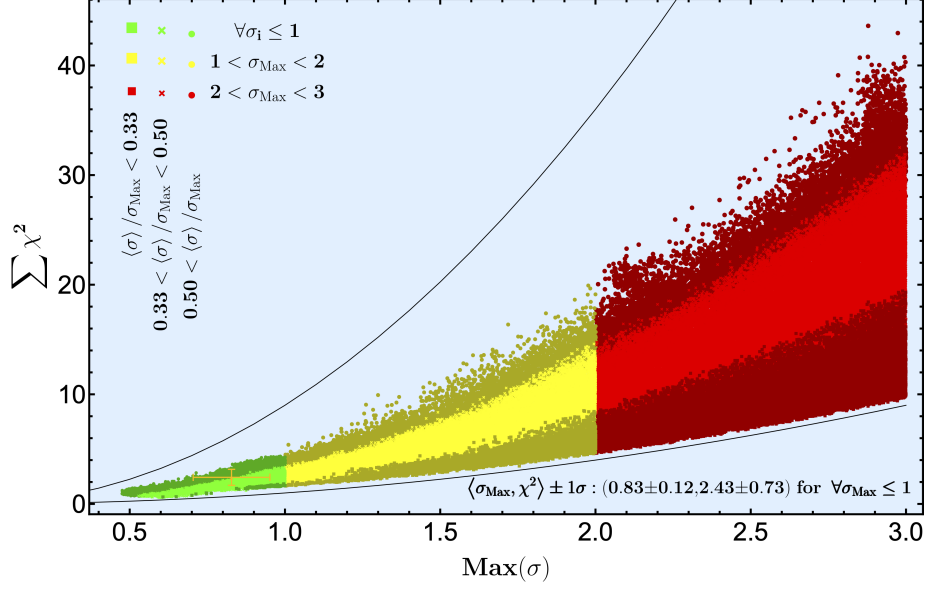


Figure 5: A plot of the distribution of model global fit vs maximum deviation (up to 3σ). The theoretical upper and lower bounds are represented by solid curves, and the mean value is denoted by $\langle \rangle$.

6 Discussion

The plots shown in the previous section, Figs. 2 and 4, can be used to identify and determine the reasons of varying levels of correlation between parameters and observable variables. As expected, the γ and β parameters have an effect on the mass values of quarks in the up and down sectors. For example, γ_u is expected to be strongly correlated with m_u , and m_c and m_t are expected to be weakly correlated. However, because β_u is about 70 times bigger than γ_u , the strong correlation of γ_u with m_u is blurred into medium level due to β_u interference. β_u , as predicted, has a strong correlation with m_c and m_t . It has a little effect on m_u due to the relative size of β_u in comparison to γ_u . The presence of BSM heavy isosinglet quarks (henceforth the *BSM effect*), is another factor in determining the masses of the SM up sector quarks. This effect is governed in the model by the input parameter ε , which is the dominant influence parameter on the m_t mass and in the limit ε approaches one m_t vanishes.

On the other hand, the situation differs drastically for the down sector of the SM. γ_d and m_d are correlated on a medium level, much like the up sector. The leading effect of β_d results in a subdominant correlation between γ_d and the heavier down quark mass eigenvalues (m_s and m_b). Correlation of β_d with m_d , m_s , and m_b is enhanced proportionally to the mass of the down sector quark, because the effect of γ_d becomes less apparent with larger mass of the quark. Since there is no BSM effect in strong contrast with the up SM sector, lighter mass eigenvalues', *e.g.* m_d , dependence is lead by γ_d , whereas larger mass eigenvalues', *e.g.* m_b , dependence is dominated by β_d .

Regarding the CKM mixing angles, only the $\sin(\theta_{23}^{\text{CKM}})$ has a correlation pattern with γ_d, β_d input parameters and down sector SM quark masses. The correlation of other CKM mixing angles with input parameters or SM quark masses is much weaker or not observed at all.

As previously stated, CP violating phases are not taken into account in the present paper and left for consideration elsewhere. As a result, the elements of the mass matrices are selected to be real numbers. Therefore, some of the eigenvalues of mass matrices and some elements of the CKM matrix are obtained as negative. By adding phase multipliers to the democratic mass matrix elements, these negative signs can be removed and correct CP violating phases can be obtained. These multipliers are expected to help determine the values of χ^2 and σ_{max} as close to zero as possible. The effect of the phases on the quark masses and CKM mixing angles will be further investigated in the future.

7 Conclusion

The utilization of the DMM technique to the quark sector of the $SU(6)$ symmetry motivated 331 model Variant-B is the subject of current work. Model stands out as one of the simplest extensions of SM. Using a total of ten parameters, the quark masses and mixing angles can be obtained within one standard deviation of the experimental values. A set of three parameters (a, γ, β) primarily control each quark sector (up, down and isosinglet up). In addition, one of the three parameters controls how SM and BSM isosinglet up type quarks are mixed. Therefore, all masses and mixing angles of SM and BSM isosinglet quarks are successfully predicted. There are a total of eighteen observable variables, nine of which are SM variables.

The best fit benchmark points are obtained by performing detailed analysis. It is found that, the best fit point is the point with the lowest $\chi^2 = 0.668$ and the maximum standard deviation 0.611 from the experimental value, which is corresponding to m_u . The other critical benchmark point is the one which has the lowest achievable error of standard deviation from the experimental data, with a $\chi^2 = 1.257$ value and the lowest maximum deviation of 0.487. Besides producing the point with mean value for all created data set with the $\sigma_{\text{max}} \leq 1$ condition, the plot summarizing all the data set in σ_{max} vs χ^2 graph is also generated.

In our previous paper, the democratic parameterization Variant-A of 331 model has succeeded in guiding us to the SM quark masses and hierarchy between them in accordance with the recent experimental data. Among the goals of this study, is to confirm that the parameterization at hand is valid for the Variant-B as well. The current work proves that SM quark masses and hierarchy among them are capable of being produced successfully via the democratic parameterization. Additionally, CKM mixing angles are also obtained within appropriate experimental limits. This leads us to a conclusion that further studies on altered parameter schemes based on fundamental democratic pattern are well motivated. Future research should examine UV models of flavor symmetry that naturally lead to democratic based scheme of quark mass sector. Conclusion drawn from the foregoing is that this may also provide a solution to the hierarchy problem.

Acknowledgments

RC was supported by Ege University Scientific Research Projects Coordination under Grant Number FGA-2021-22954. OP was supported by the Samsung Science and Technology Foundation under Grant No. SSTF-BA1602-04 and National Research Foundation of Korea under Grant Number 2018R1A2B6007000.

References

- [1] S. M. Boucenna, S. Morisi and J. W. F. Valle, *Radiative neutrino mass in 3-3-1 scheme*, *Phys. Rev. D* **90** (2014) 013005 [[1405.2332](#)].
- [2] M. B. Tully and G. C. Joshi, *Generating neutrino mass in the 331 model*, *Phys. Rev. D* **64** (2001) 011301 [[hep-ph/0011172](#)].
- [3] N. T. Duy, P. N. Thu and D. T. Huong, *New physics in $b \rightarrow s$ transitions in the MF331 model*, *2205.02995*.
- [4] A. Addazi, G. Ricciardi, S. Scarlatella, R. Srivastava and J. W. F. Valle, *An old theme for new data: Interpreting recent B anomaly data within an extended 331 gauge theory*, *2201.12595*.
- [5] A. J. Buras, F. De Fazio and J. Girrbach, *331 models facing new $b \rightarrow s\mu^+\mu^-$ data*, *JHEP* **02** (2014) 112 [[1311.6729](#)].
- [6] A. J. Buras, F. De Fazio, J. Girrbach and M. V. Carlucci, *The Anatomy of Quark Flavour Observables in 331 Models in the Flavour Precision Era*, *JHEP* **02** (2013) 023 [[1211.1237](#)].
- [7] M. Singer, J. W. F. Valle and J. Schechter, *Canonical Neutral Current Predictions From the Weak Electromagnetic Gauge Group $SU(3) \times U(1)$* , *Phys. Rev. D* **22** (1980) 738.
- [8] F. Pisano and V. Pleitez, *An $SU(3) \times U(1)$ model for electroweak interactions*, *Phys. Rev. D* **46** (1992) 410 [[hep-ph/9206242](#)].
- [9] P. H. Frampton, *Chiral dilepton model and the flavor question*, *Phys. Rev. Lett.* **69** (1992) 2889.
- [10] M. Reig, J. W. F. Valle and C. A. Vaquera-Araujo, *Unifying left-right symmetry and 331 electroweak theories*, *Phys. Lett. B* **766** (2017) 35 [[1611.02066](#)].
- [11] H. N. Long, *The 331 model with right handed neutrinos*, *Phys. Rev. D* **53** (1996) 437 [[hep-ph/9504274](#)].
- [12] A. E. Carcamo Hernandez, R. Martinez and F. Ochoa, *Z and Z' decays with and without FCNC in 331 models*, *Phys. Rev. D* **73** (2006) 035007 [[hep-ph/0510421](#)].
- [13] J. T. Liu and D. Ng, *Lepton flavor changing processes and CP violation in the 331 model*, *Phys. Rev. D* **50** (1994) 548 [[hep-ph/9401228](#)].
- [14] S. Profumo and F. S. Queiroz, *Constraining the Z' mass in 331 models using direct dark matter detection*, *Eur. Phys. J. C* **74** (2014) 2960 [[1307.7802](#)].
- [15] A. E. Cárcamo Hernández, R. Martinez and F. Ochoa, *Fermion masses and mixings in the 3-3-1 model with right-handed neutrinos based on the S_3 flavor symmetry*, *Eur. Phys. J. C* **76** (2016) 634 [[1309.6567](#)].
- [16] R. M. Fonseca and M. Hirsch, *A flipped 331 model*, *JHEP* **08** (2016) 003 [[1606.01109](#)].

- [17] CDF collaboration, T. Aaltonen et al., *High-precision measurement of the W boson mass with the CDF II detector*, *Science* **376** (2022) 170.
- [18] M. C. Rodriguez, *The W -boson mass anomaly and Supersymmetric $SU(3)_C \otimes SU(3)_L \otimes U(1)_N$ Model*, *2205.09109*.
- [19] A. E. Carcamo Hernandez, R. Martinez and F. Ochoa, *Radiative seesaw-type mechanism of quark masses in $SU(3)_C \otimes SU(3)_L \otimes U(1)_X$* , *Phys. Rev. D* **87** (2013) 075009 [[1302.1757](#)].
- [20] A. E. Cárcamo Hernández, E. Cataño Mur and R. Martinez, *Lepton masses and mixing in $SU(3)_C \otimes SU(3)_L \otimes U(1)_X$ models with a S_3 flavor symmetry*, *Phys. Rev. D* **90** (2014) 073001 [[1407.5217](#)].
- [21] A. E. Cárcamo Hernández, S. Kovalenko, H. N. Long and I. Schmidt, *A variant of 3-3-1 model for the generation of the SM fermion mass and mixing pattern*, *JHEP* **07** (2018) 144 [[1705.09169](#)].
- [22] E. R. Barreto, A. G. Dias, J. Leite, C. C. Nishi, R. L. N. Oliveira and W. C. Vieira, *Hierarchical fermions and detectable Z' from effective two-Higgs-triplet 3-3-1 model*, *Phys. Rev. D* **97** (2018) 055047 [[1709.09946](#)].
- [23] F. F. Deppisch, C. Hati, S. Patra, U. Sarkar and J. W. F. Valle, *331 Models and Grand Unification: From Minimal $SU(5)$ to Minimal $SU(6)$* , *Phys. Lett. B* **762** (2016) 432 [[1608.05334](#)].
- [24] C. Kownacki, E. Ma, N. Pollard, O. Popov and M. Zakeri, *Dark revelations of the $[SU(3)]^3$ and $[SU(3)]^4$ gauge extensions of the standard model*, *Phys. Lett. B* **777** (2018) 121 [[1710.00762](#)].
- [25] C. Kownacki, E. Ma, N. Pollard, O. Popov and M. Zakeri, *Alternative $[SU(3)]^4$ model of leptonic color and dark matter*, *Nucl. Phys. B* **928** (2018) 520 [[1801.01379](#)].
- [26] A. Alves, G. Arcadi, P. V. Dong, L. Duarte, F. S. Queiroz and J. W. F. Valle, *Matter-parity as a residual gauge symmetry: Probing a theory of cosmological dark matter*, *Phys. Lett. B* **772** (2017) 825 [[1612.04383](#)].
- [27] P. V. Dong, D. T. Huong, F. S. Queiroz, J. W. F. Valle and C. A. Vaquera-Araujo, *The Dark Side of Flipped Trinification*, *JHEP* **04** (2018) 143 [[1710.06951](#)].
- [28] S. K. Kang, O. Popov, R. Srivastava, J. W. F. Valle and C. A. Vaquera-Araujo, *Scotogenic dark matter stability from gauged matter parity*, *Phys. Lett. B* **798** (2019) 135013 [[1902.05966](#)].
- [29] J. Leite, O. Popov, R. Srivastava and J. W. F. Valle, *A theory for scotogenic dark matter stabilised by residual gauge symmetry*, *Phys. Lett. B* **802** (2020) 135254 [[1909.06386](#)].
- [30] R. Ciftci, A. K. Ciftci and O. Popov, *New parameterization and analysis for E_6 inspired 331 model*, *2211.16529*.
- [31] L. A. Sanchez, W. A. Ponce and R. Martinez, *$SU(3)_c \times SU(3)_\ell \times U(1)_X$ as an $E(6)$ subgroup*, *Phys. Rev. D* **64** (2001) 075013 [[hep-ph/0103244](#)].
- [32] A. Hartanto and L. T. Handoko, *Grand unified theory based on the $SU(6)$ symmetry*, *Phys. Rev. D* **71** (2005) 095013 [[hep-ph/0504280](#)].
- [33] R. Martínez, W. A. Ponce and L. A. Sánchez, *$SU(3)_c \otimes SU(3)_L \otimes U(1)_X$ as an $SU(6) \otimes U(1)_X$ subgroup*, *Phys. Rev. D* **65** (2002) 055013 [[hep-ph/0110246](#)].

- [34] W. A. Ponce, J. B. Florez and L. A. Sanchez, *Analysis of $SU(3)_c \times SU(3)_L \times U(1)_X$ local gauge theory*, *Int. J. Mod. Phys. A* **17** (2002) 643 [[hep-ph/0103100](#)].
- [35] H. Fritzsch, Z.-z. Xing and D. Zhang, *Correlations between quark mass and flavor mixing hierarchies*, *Nucl. Phys. B* **974** (2022) 115634 [[2111.06727](#)].
- [36] PARTICLE DATA GROUP collaboration, P. Zyla et al., *Review of Particle Physics*, *PTEP* **2020** (2020) 083C01.
- [37] G. Aad, B. Abbott, D. Abbott, O. Abidinov, A. Abed Abud, K. Abeling et al., *Search for high-mass dilepton resonances using 139 fb⁻¹ of pp collision data collected at $\sqrt{s} = 13$ TeV with the atlas detector*, *Physics Letters B* **796** (2019) 68.
- [38] CMS collaboration, C. Collaboration, *Search for a narrow resonance in high-mass dilepton final states in proton-proton collisions using 140 fb⁻¹ of data at $\sqrt{s} = 13$ TeV*, tech. rep., CERN, Geneva, 2019.
- [39] ATLAS collaboration, G. Aad, B. Abbott, D. C. Abbott, O. Abidinov, A. Abed Abud, K. Abeling et al., *Search for a heavy charged boson in events with a charged lepton and missing transverse momentum from pp collisions at $\sqrt{s} = 13$ TeV with the atlas detector*, *Phys. Rev. D* **100** (2019) 052013.
- [40] H. Harari, H. Haut and J. Weyers, *Quark masses and cabibbo angles*, *Physics Letters B* **78** (1978) 459.
- [41] H. Fritzsch, *Quark masses and flavor mixing*, *Nuclear Physics B* **155** (1979) 189.
- [42] H. Fritzsch, *Hierarchical chiral symmetries and the quark mass matrix*, *Physics Letters B* **184** (1987) 391.
- [43] H. Fritzsch and J. Plankl, *Flavour democracy and the lepton-quark hierarchy*, *Physics Letters B* **237** (1990) 451.
- [44] H. Fritzsch and D. Holtmannspötter, *The breaking of subnuclear democracy as the origin of flavour mixing*, *Physics Letters B* **338** (1994) 290.
- [45] A. Datta and S. Raychaudhuri, *Quark masses and mixing angles in a four-generation model with a naturally heavy neutrino*, *Phys. Rev. D* **49** (1994) 4762.
- [46] A. Çelikel, A. K. Çiftçi and S. Sultansoy, *A search for the fourth SM family*, *Physics Letters B* **342** (1995) 257.
- [47] A. Djouadi and A. Lenz, *Sealing the fate of a fourth generation of fermions*, *Physics Letters B* **715** (2012) 310.
- [48] C. Collaboration, S. Basegmez, G. Bruno, R. Castello, L. Ceard, C. Delaere et al., *Searches for higgs bosons in pp collisions at $\sqrt{s} = 7$ and 8 TeV in the context of four-generation and fermiophobic models*, *Phys. Lett* **725** (2013) 36.
- [49] S. Atağ, A. Çelikel, A. K. Çiftçi, S. Sultansoy and U. O. Yilmaz, *Fourth SM family, breaking of mass democracy, and the CKM mixings*, *Phys. Rev. D* **54** (1996) 5745.
- [50] A. K. Çiftçi, R. Çiftçi and S. Sultansoy, *Search for the fourth standard model family fermions and E_6 quarks at $\mu^+\mu^-$ colliders*, *Phys. Rev. D* **65** (2002) 055001.
- [51] A. K. Çiftçi, R. Çiftçi and S. Sultansoy, *Fourth standard model family neutrino at future linear colliders*, *Phys. Rev. D* **72** (2005) 053006.
- [52] R. Çiftçi and A. K. Çiftçi, *General structure of democratic mass matrix of quark sector in E_6 model*, *AIP Conf. Proc.* **1722** (2016) 070004.